Bioorganic & Medicinal Chemistry xxx (2015) xxx–xxx

Contents lists available at ScienceDirect

Bioorganic & Medicinal Chemistry

journal homepage: www.elsevier.com/locate/bmc

Imine/amide–imidazole conjugates derived from 5-amino-4-cyano-*N*1-substituted benzyl imidazole: Microwave-assisted synthesis and anticancer activity via selective topoisomerase-II-α inhibition

Arvind Negi [a], Jimi Marin Alex [a], Suyog M. Amrutkar [c], Ashish T. Baviskar [c], Gaurav Joshi [a], Sandeep Singh [b], Uttam C. Banerjee [c], Raj Kumar [a,*,†]

[a] Laboratory for Drug Design and Synthesis, Centre for Chemical and Pharmaceutical Sciences, Central University of Punjab, 151 001 Bathinda, India
[b] Centre for Genetic Diseases and Molecular Medicine, Central University of Punjab, 151 001 Bathinda, India
[c] Department of Pharmaceutical Technology (Biotechnology), National Institute of Pharmaceutical Education and Research (NIPER), Mohali, S.A.S. Nagar, Sec 67, 160 062 Punjab, India

ARTICLE INFO

Article history:
Received 26 May 2015
Revised 9 July 2015
Accepted 10 July 2015
Available online xxxx

Keywords:
Imine/amide–imidazole
Anticancer activity
Topoisomerase inhibition
Antioxidant activity
Molecular modeling

ABSTRACT

Microwave-accelerated synthesis and anticancer activity of novel imine/amide–imidazole conjugates derived from 5-amino-4-cyano-*N*1-substituted benzyl imidazole against a panel of seven cancer cell lines are reported for the first time. Compounds **ARK-4**, **10** and **12** in the series show promising in vitro anti proliferative activity with low micromolar IC_{50} values against A-459 (lung), Hep-G2 (liver) and H-460 (liver) cancer cell lines. Compounds caused the increase in ROS levels as well as mitochondrial membrane depolarization, which might induce apoptosis. Further, mechanistic interventions on biological and molecular modeling data supported that compounds inhibited topoisomerase-II selectively.

1. Introduction

Cancer represents a group of more than hundred diseases characterized by uncontrolled proliferation of the cells.[1] According to WHO, cancer deaths are predicted to rise with an approximation of 13.1 million deaths in the year 2030 worldwide. Despite availability of various anticancer drugs, the problems like less therapeutic efficacy with prevailing agents due to multi-drug resistance, adverse effects and/or poor bioavailability warrant anticancer screening of new chemical entities. Persistent failure in anticancer drug development prompted the researchers to use the strategies of combining pharmacophores as targeted therapeutic agents.[2] These drugs have the potential to overcome the fast development of resistance, enhance patient compliance, and reduce both the cost and the risk of drug–drug interactions.[3] The scope of molecular hybridization can be clearly exemplified through the US-FDA approved estramustine and successful ongoing of other hybrid molecules that are currently in different phases of clinical trials such as CUDC-101, CBLC-137, PLX3397, E-3810, and CUDC-907.[2] In continuation of our previous efforts towards anticancer drug discovery[4–9] and development,[10] we thought of designing hybrid pharmacophores derived from imine–imidazoles and imine–amides (Fig. 1) in which one of the aromatic rings of stilbenes[11,12]/imines (**1**) or benzamides (**2**) was substituted with imidazole scaffold, that is, 5-amino-4-cynao-*N*1-substituted benzyl imidazole (**3**). This is anticipated to solve the issue of limited bioavailability due to glucuronidation and sulfation as observed with most of stilbenes and offer an alternative strategy other than acetylation[13] and methylation.[14] Also the designed compounds may be expected to exhibit better anticancer activity of benzamides which are reported to show their anticancer effect either via inhibition of protein tyrosine kinases,[15] PI3K,[16] histone deacetylase,[17,18] tubulin[19] or DNA methylation.[20]

2. Results and discussion

2.1. Synthesis

Compound **3** as an intermediate for the synthesis of the target compounds **ARK-4–13** was prepared by using synthetic procedures shown in Scheme 1. Briefly 2,3-diaminomaleonitrile was treated with $CH(OEt)_3$ in 1,4-dioxane to afford ethyl (*Z*)-*N*-(2-amino-1,2-dicyanovinyl)formimidate (**4**) which on reaction with

* Corresponding author. Tel.: +91 164 2430586; fax: +91 164 2240555.
E-mail addresses: raj.khunger@gmail.com, rajcps@cup.ac.in (R. Kumar).
† CUPB Library Communication Number P007/15.

http://dx.doi.org/10.1016/j.bmc.2015.07.020
0968-0896/

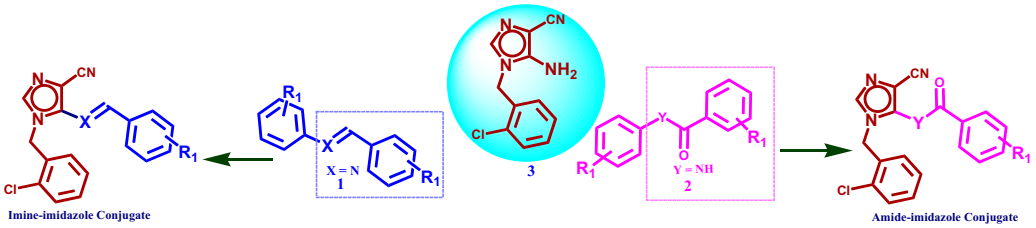

Figure 1. Design of target compounds.

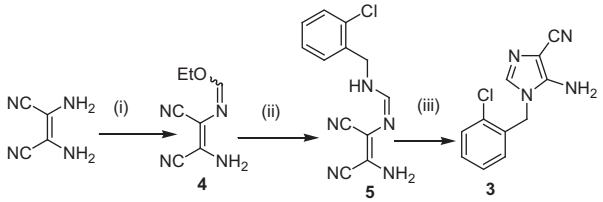

Scheme 1. Reagents and conditions: (i) $CH(OEt)_3$, dry 1,4-dioxane, reflux, 8–10 h; (ii) *o*-Cl-$PhCH_2NH_2$, EtOH, aniline hydrochloride (1 mol %), rt, 5–6 h; (iii) 1 M KOH, rt, 7–8 h.

o-chlorobenzylamine under the catalytic influence of aniline hydrochloride in ethanol furnished *N′*-((*Z*)-2-amino-1,2-dicyanovinyl)-*N*-(2-aminophenyl)formimidamide (**5**). Cyclization of **4** under the influence of base resulted in the formation of 1-(2-chlorobenzyl)-5-amino-1*H*-imidazole-4-carbonitrile (**3**), which acted as the precursor for the formation of target compounds.[21,22]

2.2. Optimization of the reaction conditions for the synthesis of imine–imidazole and amide–imidazole hybrids

Microwave (MW) assisted organic synthesis[23–26] is swiftly advancing and is now accepted as a valuable tool to overcome some of the bottlenecks in the drug discovery process and has enhanced the rapid generation of libraries of compounds in lesser time, high yields, proficient and speedy dielectric heating of the reaction mixture in a conserved vessel to temperatures even higher than the boiling point of the solvent.[6,27]

In order to determine the optimum reaction conditions for the synthesis of imine–imidazole hybrids (**ARK-4**–**11**), a representative reaction of **3** (1 equiv) was carried out with 4-hydroxybenzaldehyde (1 equiv) under various MW reaction conditions. The results are summarized in Table 1. The best results were obtained in carrying out reaction in methanol for 15 min TLC at 120 °C under MW irradiation. The very low yield and higher time required under conventional heating could be due to poor nucleophilicity of amino group because of delocalization of its lone pair in conjugation with adjacent nitrile group.

2.3. Synthesis of imine–imidazole and amide–imidazole hybrids

Utilizing this standardized reaction condition, **3** (1 equiv) was condensed under MW irradiations with various aryl aldehydes (1 equiv) in methanol to furnish the imine–imidazole conjugates compounds (**ARK-4**–**11**; Scheme 2). Furthermore, two amide–imidazole conjugates (**ARK-12**–**13**) were synthesized (Scheme 3) by treating **3** (1 equiv) with acetic or benzoic anhydrides (1 equiv) under MW heating.

The reactions were found to be compatible with aromatic aldehydes bearing electron withdrawing and donating substituents. Imine–imidazole conjugates precipitated and were removed from

Table 1
Standardization of the reaction conditions for the syntheses of (*E*)-1-(2-chlorobenzyl)-5-((4-hydroxybenzylidene)amino)-1*H*-imidazole-4-carbonitrile (**ARK-8**)

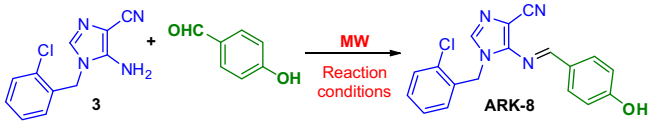

Entry	Solvent	Temp (°C)	Time (h)	Yield[a,b]
1	—	120	1	12[c]
2	Toluene[d]	80	1.5	85
3	Toluene[d]	120	1.5	89
4	NMP[d]	80	1.5	82
5	NMP[d]	120	1.5	84
6	MeOH[d]	80	20 min	85
7	MeOH[d]	120	15 min	88
8	H_2O[d]	80	3	63
9	H_2O[d]	120	3.5	72
10	DMF[d]	80	1.7	77
11	DMF[d]	120	1.9	79

[a] A stirred mixture of **3** (1 mmol) and 4-hydroxybenzaldehyde (1 equiv) in a sealed vial was heated under microwave irradiations using Biotage Initiator.
[b] Isolated yield.
[c] Trace amount of product was obtained in carrying out the reaction under conventional heating at 80 °C for 12 h.
[d] 0.5 mL of solvent was used.

methanol and purified (72–93%) through recrystallization (methanol). The amide–imidazoles obtained after aqueous work-up were dried, and recrystallized (methanol). All the target compounds were found to be new and fully characterized by ^1H and ^{13}C NMR, IR, and HRMS data. The appearance of IR absorption frequencies in range of 1642–1688 cm^{-1} (C=N str.), singlet at range of 8.4–9.7 δ in ^1H NMR spectra due to –N=C*H*– and peak in the range of 160–165 δ in case of ^{13}C NMR and mass spectra confirmed the formation of imine–imidazole hybrids (**ARK-4**–**11**). The melting points for these compounds were observed to be in the range of 167–204 °C. The melting points for **ARK-12** and **ARK-13** were found to be in the range of 192–194 °C and 231–235 °C, respectively.

Since imines can have two configurational isomers, that is, *E* and *Z*, and we obtained single isomer (TLC, NMR), we were interested to know which isomer we are dealing with. We utilized the structure minimization tool of ChemBio3D Ultra licensed version (Licenced@ Cambridge-soft) for finding out the stability of isomers. **ARK-4** was selected as it has more substituents which could be profoundly effective in determining the configurations based on quantum theories. The MMFF94X force-field calculations supported that *E*-isomer was found to be more stable (Fig. 2a) in comparison to the *Z* (Fig. 2b) based on parameters collected in Table 2. Further, *Z*-isomer suffers steric clashes which could be easily determined by observing the torsional and total energy level.

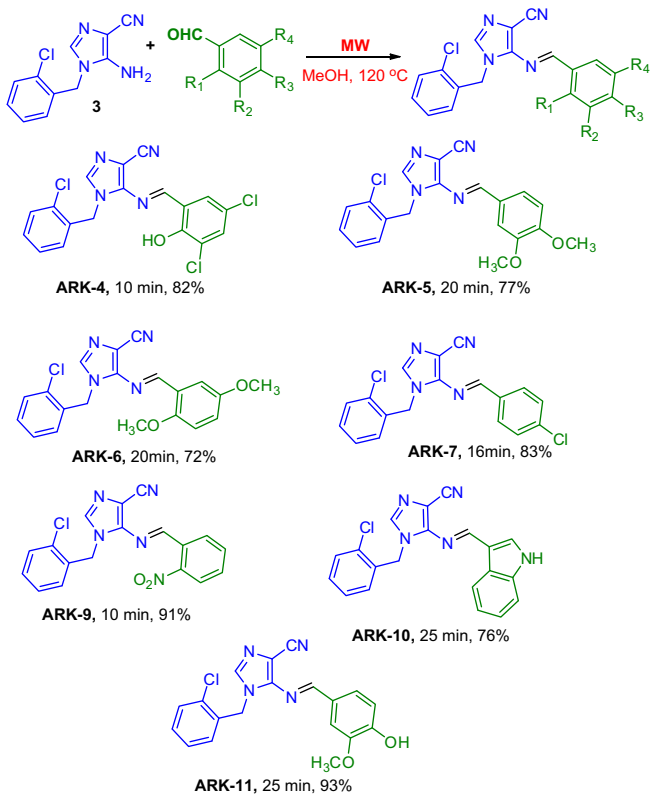

Scheme 2. Synthesis of target compounds (**ARK-4**–**11**).

2.4. Biological studies

2.4.1. Antiproliferative activity

In order to determine the antiproliferative potential of the target compounds **ARK-4**–**13** were screened in vitro against a panel of seven cancer cell lines, comprising of A-459 (lung), Hep-G2 (liver), H-460 (liver), HeLa (cervix), MCF7 (breast), PC3 (prostate) and IGROV-1 (ovary). Overall all the tested compounds exhibited the antiproliferative effects in only three cell lines (results in other cancer cell lines not shown), A-459 (lung), Hep-G2 (liver) and H-460 (liver); the results are summarized in Table 3. The compounds **ARK-4**, **ARK-10** and **ARK-12** showed significant in vitro anticancer activity in A-459, Hep-G2 and H-460 cancer lines. Etoposide (Etop)[28] was used as the positive control. The compounds did not show significant cytotoxicity towards human peripheral blood cells (hPBMCs) that served as normal control.

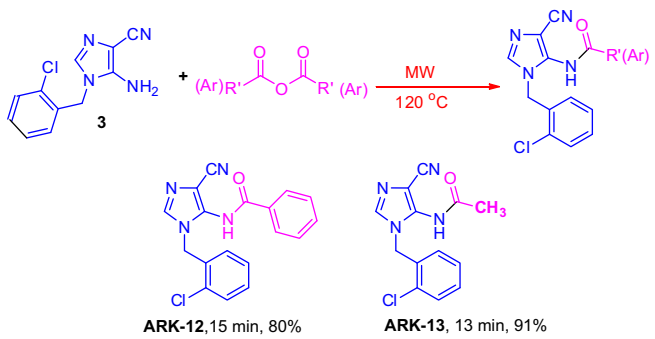

Scheme 3. Synthesis of target compounds (**ARK-12**–**13**).

2.4.2. Reactive oxygen species (ROS) and mitochondrial membrane integrity assays

Anticancer activity of most of the compounds is mediated through changes in the ROS status in the cell. To evaluate mode of action of our investigational compounds the ROS study using DHE based fluorescent detection system has been performed. In this study **ARK-4** was selected as representative compound. The results showed that there is concentration dependent increase in ROS levels in the treated cells (Fig. 3A). Increase in ROS levels is generally associated with changes in mitochondrial membrane potential,[5] which triggers its depolarization and lead to release of cytochrome-c into cytoplasm, thus inducing apoptosis. JC-1 dye was used to measure membrane potential of the mitochondria (Fig. 3B), the results showed that there is steady decrease in OD590/OD527 ratio indicating increased mitochondrial membrane depolarization.

2.4.3. TopoII-mediated DNA decatenation assay

Since many of the imidazole, its fused derivatives[29,30] and imines[4] are known to present anticancer activity via obstructing the activity of topoisomerases (Topo) I and or IIα, we planned to evaluate some of the selected compounds of ARK series (**ARK-4**, **6**–**10**, **12** and **13**) for their ability to inhibit them.

To assess the activity against topoisomerase (hTopo) IIα, the synthetics were subjected to ATP-dependent decatenation assay in agarose gel electrophoresis (Fig. 4), a specific assay for the topoisomerase II inhibition activity. In this assay kinetoplast DNA (kDNA) was used as a substrate and etoposide, a known topoisomerase II-inhibiting anticancer drug, was used as standard.

Two decatenated products: nicked kDNA (Nck) and supercoiled (SC)/relaxed (Rel) circular DNA were obtained on incubation of kDNA with hTopoIIα. Quantification of decatenation products formed (Nck, Rel, and SC) were carried out by densitometric data obtained using Quantity One (BioRad), and the results were compared with etoposide. As expected, compounds **ARK-4**, **10** and **12** were observed to be more active against hTopoIIα. **ARK-4**, **10** and **12** exhibited greater inhibition of hTopoIIα activity as

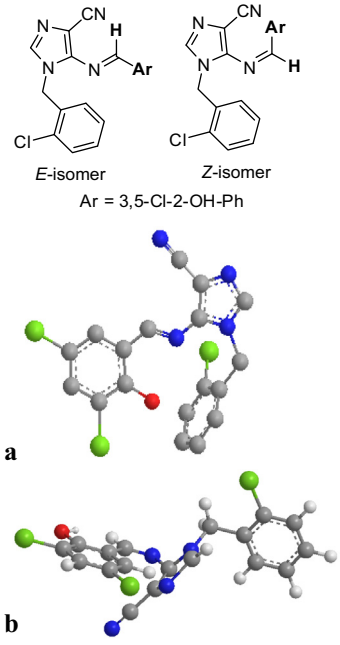

Figure 2. (a) (*E*)-1-(2-Chlorobenzyl)-5-((3,5-dichloro-2-hydroxybenzylidene)amino)-1*H*-imidazole-4-carbonitrile, (b) (*Z*)-1-(2-chlorobenzyl)-5-((3,5-dichloro-2-hydroxybenzylidene)amino)-1*H*-imidazole-4-carbonitrile.

Table 2
Comparison of stabilities of *E* and *Z* isomers of **ARK-4**

	E-Configuration	*Z*-Configuration
Stretch	1.4071	1.4532
Bend	23.6455	27.4343
Stretch–Bend	−0.0180	0.0594
Torsion	−13.3402	1.9418
Non-1,4 VDW	−3.2550	−5.2978
1,4 VDW	18.4778	17.8784
Dipole/dipole	−0.2708	−0.0291
Total energy	26.6465 kcal/mol	43.4402 kcal/mol

compared to etoposide (Fig. 4A and B). This study indicated that the inhibition of hTopoIIα was the putative mode of action of ARK series. The calculated IC_{50} value (Fig. 5 and also see Supplementary information) for one of the representatives of ARK series, **ARK-4** was observed to be 34.93 μM which was better than etoposide (IC_{50} = 78.4 μM).

2.4.4. Redefining selectivity of ARK-4 as hTopoIIα inhibitor

In order to assess the potential of the compounds to inhibit TopoI, we tested the **ARK-4** in TopoI relaxation assay which showed no significant inhibition of hTopoI as compared to camptothecin (C), a known TopoI inhibitory anticancer agent (Fig. 6). This indicated that the compounds represent a class of selective TopoIIα inhibitors.

2.5. Molecular modeling

In order to investigate the binding mode of the tested compounds with the active site of TopoIIα (PDB entry: 1ZXM),[31] we selected **ARK-4**, which emerged to be a potent catalytic inhibitor of TopoIIα. Molecular docking study of **ARK-4** was done using Maestro 9.6 module in Schrodinger. Molecular docking protocol was validated by docking ANP (bound ligand) into the crystal structure of ATPase domain of TopoII α. The docked ANP showed similar binding pose as the co-crystallized ligand with a root mean square deviation (rmsd) of about 0.024 Å. The binding model of ANP with ATPase domain of TopoIIα revealed that the amino group of adenine moiety showed hydrogen bonding with ASN120 and the two hydroxyl groups of ribose unit showed hydrogen bond interaction with Ser149. The oxygen atoms in the three phosphate groups displayed hydrogen bond interactions with the nitrogen atom of the Walker A motif residues; ARG 162, ASN 163, TYR 165 and GLY 166. In addition, these phosphate groups showed hydrogen bonding with ASN 91, LYS 168, and GLN 376. The highly conserved Walker A motif in the ATP binding site of TopoII α includes the residues 161–166 and these are considered crucial for the binding of ATP and other catalytic inhibitors acting on ATPase domain.[4] Further studies revealed that **ARK-4** might bind at the ATP site of TopoII α. The superimposition of the co-crystallized ANP and ARK-4 indicated that the 2-chlorobenzyl ring (ring-C) overlapped with the phosphate group of ANP in the ATP binding site (Fig. 7a). The interaction model of the most active compound **ARK-4** at the ATPase domain (Fig. 7b) showed that the hydroxyl group of 3,5-dichloro-2-hydroxybenzyl moiety (ring-A) formed a H-bond with the water molecule present at the binding site (d = 2.13 Å). Further, ring-A could show polar interactions with THR 215, ASN 120 and ASN 95. The 2-chlorobenzyl ring (ring-C) was involved in the arene–cation interaction with the Mg^{2+} ion (d = 2.63 Å). Similar kind of π–cation interactions have been reported in the binding of imine–pyrazolopyrimidinones to the ATP binding site in topo-IIα.[4] The interaction with Mg^{2+} ion has been considered essential for the catalytic activity at the ATPase binding domain.[32] Additionally, this interaction led to the formation of distorted tetrahedral conformation involving Mg^{2+} ion, 2-chlorobenzyl ring (ring-C), ASN 91, and two water molecules (HOH 927 and HOH 928). These formed a stable complex which may prevent any further catalytic activity due to the Mg^{2+} ion. Thus, the molecular modeling studies suggest that **ARK-4** may act as a catalytic inhibitor by occupying the ATP binding pocket of TopoII α and showing favorable interactions with the key amino acid residues.

Table 3
Antiproliferativeactivity of the compounds under investigations (**ARK-4**–**13**)

Compound	A-549 Lung	Hep-G2 Liver	H-460 Liver
	IC_{50}[a] (μM)		
ARK-4	7.5	12	11.2
ARK-5	>50	>50	—[b]
ARK-6	18	20	28.3
ARK-7	30.8	31	28.1
ARK-8	35.1	38.2	>40
ARK-9	37	40	—[b]
ARK-10	10.9	15	14.6
ARK-11	39	>40	—[b]
ARK-12	16.5	17.1	13.4
ARK-13	20.3	28	33.9
Etop	18.2	20.9	>30

[a] Values are derived from averaging three independent experiments and each experiment was done in triplicate.
[b] Not tested.

3. Conclusion

The current study began with the development of efficient and convenient method for the synthesis of imine/amide–imidazole conjugates by condensation of 1-(2-chlorobenzyl)-5-amino-1*H*-imidazole-4-carbonitrile with aryl aldehydes or anhydrides under microwave heating in sealed tubes. The optimization of the synthetic procedure was carried out and the effect of various solvents on the condensation reaction was studied. Methanol emerged as the best suitable solvent for carrying out the reactions. Following the optimized procedure novel imine/amide–imidazole conjugates were synthesized. The synthesized compounds showed encouraging anticancer activity in vitro with low micromolar IC_{50} values compared to etoposide against lung and liver cancer cell lines tested and with almost no toxicity to normal cells. The biological experiments on representative compounds suggested that they selectively and catalytically inhibitor hTopoIIα which was further supported by molecular docking studies. In addition, compounds were found to increase ROS levels as well as mitochondrial membrane depolarization, which might induce apoptosis, independent of their Topo-II specific activity. Further detailed investigations of SARs as well as explorations of antitumor activity are presently in progress.

4. Experimental section

4.1. Chemistry

The reagents were purchased from Sigma–Aldrich, Loba Chemie Pvt. Ltd, S.D. Fine Chemicals and Sisco Research Laboratory and used without further purification. The progress of the reaction was determined by thin layer chromatography (TLC; for imine; EtOAc/*n*-hexane::1:1; for amides; EtOAc/*n*-hexane::3:2) carried out on pre-coated silica plates. Melting points were recorded on Stuart SMP—30 melting point apparatus with open glass capillary tube and are uncorrected. Infrared spectra of compounds were recorded on Bruker IR spectrophotometer at CUPB. The ^1H and

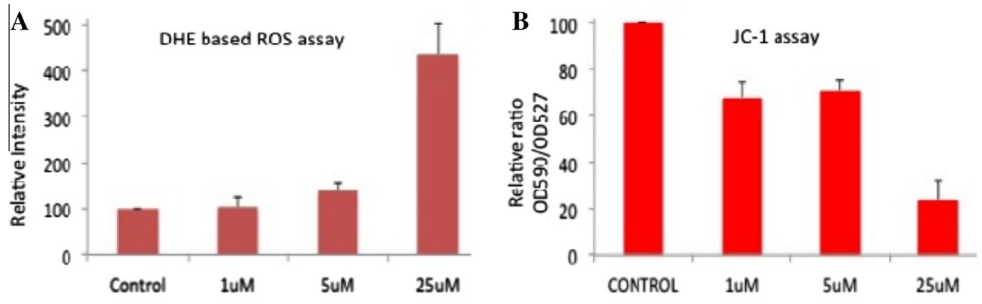

Figure 3. (A) DHE based assay to measure intra-cellular reactive oxygen species (ROS) induced by **ARK-4**. (B) JC-1 dye based assay to measure mitochondrial membrane potential altered by **ARK-4**.

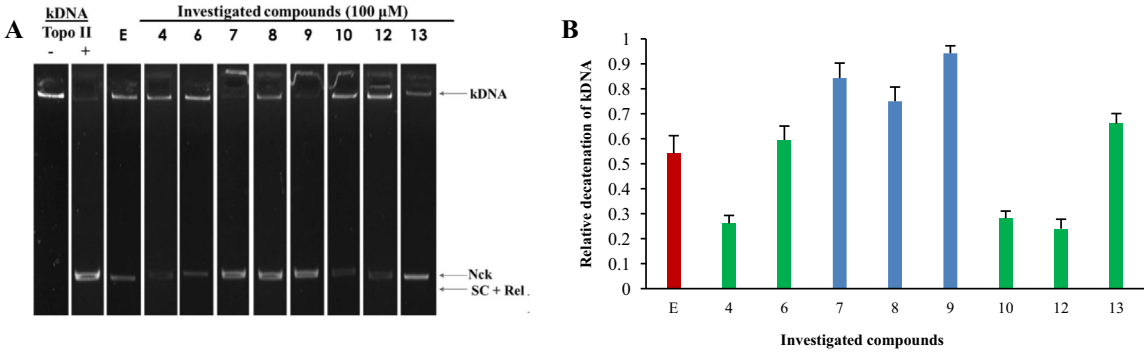

Figure 4. (A) hTopoIIα-inhibitory effect of selected ARK series compounds in kDNA decatenation assay. (B) Quantification of product formed in kDNA decatenation assay.

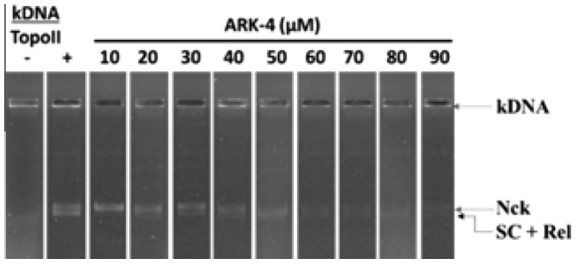

Figure 5. Determination of IC_{50} value of **ARK-4** by the inhibition of hTopoIIα catalyzed decatenation of kDNA. (Different concentrations of **ARK-4** (10–100 μM) were used.)

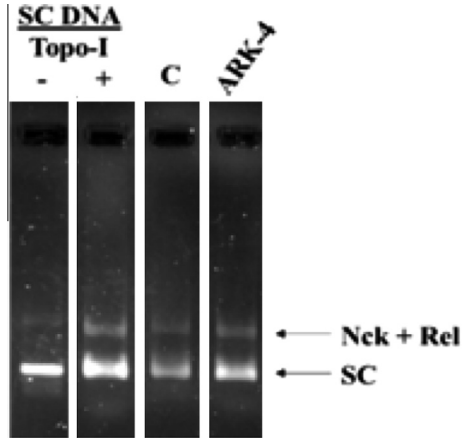

Figure 6. Topoisomerase I relaxation assay: Negatively supercoiled DNA was treated with TopoI in the presence of 100 μM camptothecin (C) or **ARK-4**, separately.

^{13}C NMR of the compounds were recorded on Bruker Advance II instrument at 400 MHz and 100 MHz frequencies, respectively, in $CDCl_3$/DMSO-d_6 and TMS ($\delta = 0$) as internal standard and HRMS at SAIF, Punjab University, Chandigarh. The solvents were evaporated on Ilmvac rotary evaporator with Julabo chiller under reduced pressure.

4.1.1. Ethyl-*N*-((*Z*)-2-amino-1,2-dicyanovinyl)formimidate (4)

A mixture of 2,3-diaminomaleonitrile (6 g, 55.5 mmol, 1 equiv) was refluxed with triethylorthoformate (9.24 mL, 55.5 mmol, 1 equiv) in dry 1,4-dioxane (25 mL) for 8–10 h after completion of the reaction (TLC), the mixture was allowed to cool overnight. The dark brown mass obtained after distilling-off 1,4-dioxane was further extracted with diethyl ether (3 × 20 mL), dried to afford **4**[21] as light brown needles (Yield: 78%). Mp 195–197 °C. IR (KBr cm^{-1}): 3309 (N–H str.), 2247 (CN str.), 2207 (CN str.), 1636 (C=N str.), 1256 (C–O str.). ^1H NMR (400 MHz, $CDCl_3$): $\delta = 7.95$ (1H, s), 4.64 (D_2O exchangeable NH_2, 2H, br s), 4.23 (q, 2H, $J = 7.3$ Hz), 1.33 (3H, t, $J = 7.3$ Hz).

4.1.2. Ethyl-*N*-((*Z*)-2-amino-1,2-dicyanovinyl)formimidate (5)

To a suspension of **4** (1.00 g, 6.09 mmol) and *o*-chlorobenzylamine (1.01 g, 6.07 mmol) in ethanol was added catalytic amount of anilinium chloride (1 mol %; 7.8 mg). The mixture was stirred at room temperature for 5–6 h (TLC). The precipitate obtained from reaction mixture was washed with diethyl ether, dried and recrystallized in absolute ethanol to afford the light brown crystals 5,[21] mp 108–110 °C (decomp.). IR (KBr cm^{-1}): 3417 (N–H str.), 2212 (CN str.), 2191 (CN str.) 1651 (C=N, str.), 1578 (N–H bend.), 741 (C–Cl str.). ^1H NMR (400 MHz, d_6-DMSO): $\delta = 8.16$ (1H, d, $J = 4.6$ Hz), 7.74 (1H, d, $J = 3.7$ Hz), 7.42–7.44 (2H, m), 7.29–7.31 (2H, m), 4.57 (2H, d, $J = 5.9$ Hz), 6.10 (D_2O exchangeable NH_2, 2H, br s).

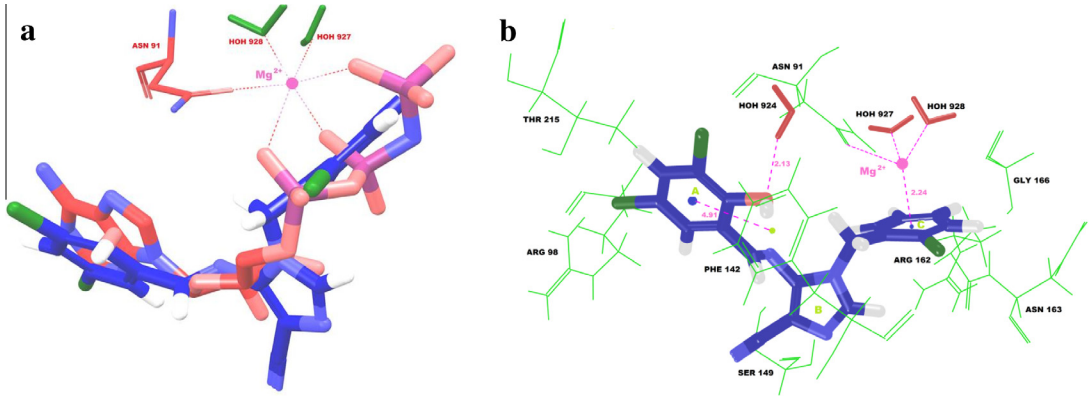

Figure 7. (a) Docking pose of **ARK-4** (red) at the binding site of AMPPNP (magenta) in ATPase domain of TopoIIα; (b) docking pose of **ARK-4** showing the interactions with important amino acid residues in ATPase domain of TopoIIα.

4.1.3. 5-Amino-1-(2-chlorobenzyl)-1*H*-imidazole-4-carbonitrile (3)

A suspension of **5** (1.00 g) in potassium hydroxide solution (1 M, 10 mL) was stirred at room temperature for approximately 7–8 h until TLC showed complete consumption of the starting material. The precipitated product was filtered-off, washed with water (5 mL), air-dried to afford the product **3**. IR (KBr cm^{-1}): 3357 (N–H str.), 2212 (CN str.), 1651 (C=N, str.), 1578 (N–H bend.), 741 (C–Cl str.). ^{1}H NMR (400 MHz, d_6-DMSO): δ = 7.50–7.52 (1H, m), 7.31–7.35 (2H, m), 7.19 (1H, s), 6.72–6.73 (1H, m), 6.32 (D_2O exchangeable NH_2, 2H, br s), 5.16 (2H, s).

4.1.4. A representative synthetic procedure of Compounds ARK-4–11

To a reaction vial, a suspension of **3** (100 mg, 0.47 mmol, 1 equiv) in methanol (0.5 mL) was added aromatic aldehyde (1 equiv) and the mixture was heated under microwave irradiation using Biotage initiator for 10–25 min at 120 °C. After the completion of reaction (TLC), methanol was removed purified through recrystallization to afford the product.

4.1.5. (*E*)-1-(2-Chlorobenzyl)-5-((3,5-dichloro-2-hydroxybenzylidene)amino)1*H*-imidazole-4-carbonitrile (ARK-4)

Yield: 82%; yellow solid; mp = 183–185 °C. IR (KBr cm^{-1}): 2250 (CN str.), 1608 (C=N str.), 1581 (C=C aromatic, str.), 1206 (C–N str.), 731 (C–Cl str.). ^{1}H NMR (400 MHz, $CDCl_3$, TMS = 0) δ: 11.35 (D_2O exchangeable OH, 1H, br s), 9.24 (1H, s), 7.9 (1H, s), 7.81 (1H, d, *J*= 2.6 Hz), 7.62 (1H, d, *J* = 2.56 Hz), 7.47 (1H, dd, $J_{1,2}$ = 1.3 Hz, $J_{1,3}$ = 7.8 Hz), 7.27–7.36 (2H, m), 7.11 (1H, dd, $J_{1,2}$ = 1.6 Hz, $J_{1,3}$ = 7.4 Hz), 5.45 (2H, s). ^{13}C NMR (100 MHz, $CDCl_3$, TMS = 0) δ: 161.73, 153.95, 145.19, 138.63, 133.26, 132.91, 132.21, 129.70, 129.51, 129.21, 128.19, 127.38, 123.79, 122.55, 122.49, 115.30, 99.85, 45.54. MS (ESI): *m*/*z* = 406 $[M+1]^+$. HRMS calcd for $C_{18}H_{11}Cl_3N_4O$ $(M+Na)^+$, 426.9891; found, 426.9912.

4.1.6. (*E*)-1-(2-Chlorobenzyl)-5-((3,4-dimethoxybenzyl idene)-amino)-1*H*-imidazole-4-carbonitrile (ARK-5)

Yield: 77%; mp = 192–194 °C; IR (KBr cm^{-1}): 2241 (CN str.), 1576 (C=N str.), 1571 (C=C aromatic, str.), 1261 (C–N str.), 731 (C–Cl str.). ^{1}H NMR (400 MHz, $CDCl_3$, TMS = 0) δ: 8.97 (1H, s), 7.52 (1H, s), 7.50 (1H, d, *J* = 1.84 Hz), 7.41–7.45 (2H, m), 7.28–7.30 (1H, m), 7.20–7.24 (1H, m), 7.11–7.14 (1H, dd, $J_{1,2}$ = 1.6 Hz, $J_{1,3}$ = 7.6 Hz), 6.95 (1H, d, *J* = 8.36 Hz), 5.37 (2H, s), 3.97 (3H, s), 3.95 (3H, s). HRMS calcd for $C_{20}H_{17}ClN_4O_2$ (M^+), 380.1040; found, 380.1051.

4.1.7. (*E*)-1-(2-Chlorobenzyl)-5-((2,5-dimethoxybenzylidene)-amino)-1*H*-imidazole-4-carbonitrile (ARK-6)

Yield: 72%; white solid. Mp = 169–171 °C. ^{1}H NMR (400 MHz, $CDCl_3$, TMS = 0) δ: 9.49 (D_2O exchangeable NH, 1H, br s), 7.57 (1H, d, *J* = 2.8 Hz), 7.52 (1H, s), 7.41–7.43 (1H, m), 7.33 (1H, d, *J* = 3.2 Hz), 7.28 (1H, d, *J* = 1.72 Hz), 7.07–7.15 (3H, m), 5.36 (2H, s), 3.80 (3H, s), 3.88 (3H, s). HRMS calcd for $C_{20}H_{17}ClN_4O_2$ (M^+), 380.1040; found, 380.1049.

4.1.8. (*E*)-5-((4-Chlorobenzylidene)amino)-1-(2-chlorobenzyl)-1*H*-imidazole-4-carbonitrile (ARK-7)

Yield: 83%; yellow solid; mp = 167–169 °C IR (KBr cm^{-1}): 2250 (CN str), 1608 (C=N str), 1581 (C=C aromatic, str.), 1206 (C–N str), 731 (C–Cl str). ^{1}H NMR (400 MHz, $CDCl_3$, TMS = 0) δ: 9.06 (1H, s), 7.87 (2H, dd, *J* = 1.8 Hz), 7.54 (1H, s), 7.48 (2H, dd, *J* = 2.24 Hz), 7.42–7.44 (1H, m), 7.27–7.31 (1H, m), 7.21–7.25 (1H, m), 7.13 (1H, dd, *J* = 1.96 Hz). ^{13}C NMR (100 MHz, $CDCl_3$, TMS = 0) δ: 45.23, 115.61, 127.20, 129.01, 129.39, 129.53, 130.50, 132.37, 133.10, 133.32, 138.05, 138.12, 146.14, 162.17. MS (ESI): *m*/*z* = 355.2 $[M+1]^+$; HRMS calcd for $C_{18}H_{12}Cl_2N_4O$ $(M+Na)^+$, 377.0331; found, 377.0410.

4.1.9. (*E*)-1-(2-Chlorobenzyl)-5-((4-hydroxybenzylidene)-amino)-1*H*-imidazole-4-carbonitrile (ARK-8)

Yield: 88%; Light yellow solid; mp = 201–203 °C; IR (KBr cm^{-1}): 2241 (CN str.), 1576 (C=N str.), 1571 (C=C aromatic str.), 1261 (C–N str.), 714 (C–Cl str.). ^{1}H NMR (400 MHz, $CDCl_3$, TMS = 0) δ: 9.78 (1H, s), 8.80 (D_2O exchangeable OH, 1H, br s), 7.72–7.74 (4H, m), 7.28–7.34 (4H, m), 5.38 (2H, s). ^{13}C NMR (100 MHz, $CDCl_3$, TMS = 0) δ: 45.02, 97.66, 115.96, 116.14, 125.96, 127.31, 129.39, 129.51, 129.57, 131.56, 132.20, 133.46, 137.57, 147.71, 162.43, 163.44; MS (ESI): *m*/*z* = 337.2 $[M+1]^+$. HRMS calcd for $C_{18}H_{13}ClN_4O_4$ $(M+Na)^+$, 359.0670; found, 359.0710.

4.1.10. (*E*)-1-(2-Chlorobenzyl)-5-((2-nitrobenzylidene)amino)-1*H*-imidazole-4-carbonitrile (ARK-9)

Yield: 91%; Pale Yellow solid; mp = 184–186 °C; IR (KBr cm^{-1}): 2198 (CN str.), 1577 (C=N str.), 1448 (C=C aromatic str.), 1256 (C–N str.), 801 (C–Cl str.); ^{1}H NMR (400 MHz, $CDCl_3$, TMS = 0) δ: 9.54 (1H, s), 8.13 (1H, dd, $J_{1,2}$ = 1.6 Hz, $J_{1,3}$ = 7.7 Hz), 8.08 (1H, dd, $J_{1,2}$ = 1.3 Hz, $J_{1,3}$ = 7.9 Hz), 7.68–7.76 (2H, m), 7.56 (1H, s), 7.43–7.47 (2H, m), 7.12 (1H, dd, $J_{1,2}$ = 1.6 Hz, $J_{1,3}$ = 7.5 Hz), 6.96 (1H, dd, $J_{1,2}$ = 1.6 Hz, $J_{1,3}$ = 7.4 Hz), 5.36 (2H, s). MS (ESI): *m*/*z* = 366.2 $[M+1]^+$. HRMS calcd for $C_{18}H_{12}ClN_5O_2$ $(M+Na)^+$, 388.0572; found, 388.0613.

4.1.11. (*E*)-5-(((1*H*-Indol-2-yl)methylene)amino)-1-(2-chlorobenzyl)-1*H*-imidazole-4-carbonitrile (ARK-10)

Yield: 76%; Brownish yellow solid mp = 167–169 °C; IR (KBr cm^{-1}): 2260 (CN str.), 1579 (C=N str.), 1559 (C=C aromatic, str.), 1198 (C–N str.), 771 (C–Cl str.). ^1H NMR (400 MHz, $CDCl_3$, TMS = 0) δ: 12.08 (1H, s), 9.05 (1H, s), 8.22 (1H, s), 8.17 (1H, d, J = 3.04 Hz), 8.0 (1H, d, J = 7.8 Hz), 7.83 (1H, s), 7.46–7.51 (2H, m), 7.22–7.33 (2H, m), 7.08–7.12 (1H, m), 7.01 (1H, dd, $J_{1,2}$ = 1.6 Hz, $J_{1,3}$ = 7.5 Hz), 5.43 (2H, s), MS (ESI): m/z = 360.2 $[M+1]^+$. HRMS calcd for $C_{20}H_{14}ClN_5$ $(M+Na)^+$, 382.0830; found, 382.0910.

4.1.12. (*E*)-1-(2-Chlorobenzyl)-5-((4-hydroxy-3-methoxybenzylidene)amino)-1*H*-imidazole-4-carbonitrile (ARK-11)

Yield: 93%; Dark yellow solid; mp = 198–200 °C; IR (KBr cm^{-1}): 2277 (CN str.), 1589 (C=N str.), 1481 (C=C aromatic, str.), 1301 (C–N str.), 778 (C–Cl str.). ^1H NMR (400 MHz, $CDCl_3$, TMS = 0) δ: 9.83 (1H, s), 8.95 (1H, s), 7.51 (1H, s), 7.41–7.45 (5H, m), 7.04 (2H, d, J = 8.48 Hz), 5.36 (2H, s), 3.97 (3H, s). MS (ESI): m/z = 367.2 $[M+1]^+$. HRMS calcd for $C_{19}H_{15}ClN_4O_2$ (M^+), 366.0884; found, 366.0781.

4.2. A representative synthetic procedure of compounds ARK-12–13

To a reaction vial, a suspension of **3** (100 mg, 0.47 mmol, 1 equiv) was added anhydride (1 equiv) and the mixture was heated under microwave irradiation using Biotage initiator for 13–15 min at 120 °C. After the completion of reaction (TLC), water was added; the precipitate was filtered off, dried and recrystallized to afford the product.

4.2.1. (*N*-(1-(2-Chlorobenzyl)-4-cyano-1*H*-imidazol-5-yl)-acetamide) (ARK-12)

Yield: 80%; white solid; mp = 192–194 °C; IR (KBr cm^{-1}): 2290 (CN str.), 1609 (C=N str.), 1341 (C=C aromatic, str.), 1213 (C–N str.), 691 (C–Cl str.). ^1H NMR (400 MHz, $CDCl_3$, TMS = 0) δ: 10.25 (D_2O exchangeable NH, 1H, br s), 7.76 (1H, s), 7.46 (2H, dd, J = 1.36 Hz), 7.29–7.37 (2H, m), 7.02 (1H, d, J = 7 Hz), 5.22 (2H, s), 2.04 (3H, s). ^{13}C NMR (100 MHz, $CDCl_3$, TMS = 0) δ: 169.18, 137.47, 135.06, 132.71, 132.30, 129.75, 129.47, 129.25, 127.39, 114.43, 107.12, 45.92, 22.36; MS (ESI): m/z = 275 $[M+1]^+$. HRMS calcd for $C_{13}H_{11}ClN_4O$ $(M+Na)^+$, 297.0514; found, 297.0612.

4.2.2. *N*-(1-(2-Chlorobenzyl)-4-cyano-1*H*-imidazol-5-yl)-benzamide (ARK-13)

Yield: 91%; light Yellow solid; mp = 231–233 °C; IR (KBr cm^{-1}): 2244 (CN str.), 1609 (C=O str.), 1510 (C=C aromatic str.), 1293 (C–N str.), 817 (C–Cl str.). ^1H NMR (400 MHz, $CDCl_3$, TMS = 0) δ: 8.30 (2H, d, J = 7.4 Hz), 7.82 (1H, s), 7.58 (1H, d, J = 7.28 Hz), 7.53 (2H, d, J = 7.84 HZ), 7.46 (2H, d, J = 4.32 Hz), 5.49 (2H, s). HRMS calcd for $C_{18}H_{12}ClN_4O$ $(M+Na)^+$, 359.0670; found, 359.0820.

4.3. Cell culture and treatment

All the cell lines were procured from National cell repository, NCCS, Pune. Cell lines representing different human cancers were grown in DMEM media supplemented with 10% fetal bovine serum (FBS) and antibiotic solution (1% Penstrip, all the reagents from Invitrogen). Cells were cultured in DMEM media with 10% FBS, 50 U/mL penicillin G, 50 Ig/mL streptomycin sulfate and 1.25 Ig/mL amphotericin B (fungizone). The cells were incubated at 37 °C with 5% CO_2 and 95% humidity conditions. For experiments, cells were seeded in equal numbers after trypan blue cell counting (8000 cells per well of 96-well plate). The compounds were dissolved in cell culture grade DMSO up to concentration of 100 mM and further dilutions were done in serum free DMEM media. The total amount of media per well (100 μL per well of 96 well plate) was kept constant and all the treatment volumes were accommodated within these ranges only.

4.3.1. 3-(4,5-Dimethythiazol-2-yl)-2,5-diphenyl tetrazolium bromide (MTT) assay

MTT assay was carried out using 96-wellplate; each well was filled by 100 μL media to which cell were treated and thereafter washed with 1% PBS and were mixed with 100 μL/mL well of MTT (5 mg in 10 mL of 1% PBS) and incubated at room temperature in dark for 4 h to allow formation of formazan crystals. Each well was then mixed with 100 μL of DMSO to dissolve the crystals followed by ELISA readings at 570 nm. The results were then represented as mean ± SD obtained from three independent experiments.

4.3.2. Reactive oxygen species (ROS) and mitochondrial membrane integrity assays

Cells were seeded in 96-well plate and appropriate treatments were given. 24 h post treatments, cells were processed for JC-1 or DHE staining. For DHE staining, cells were washed by 1× PBS followed by staining with DHE at 37 °C for 30 min. Afterwards cells were washed again with ice-cold 1× PBS and finally 100 μl of 1× PBS was added to each well followed by measuring OD using microplate reader.

For JC-1 assay, dye was directly added to the media and cells were incubated at 37 °C for 30 min followed by washing with 1× PBS to remove extra dye. OD was measured using microplate reader (emission = 527 and 590).

4.3.3. Topoisomerase inhibitory activity evaluation

All the reagents required for the testing of investigational compounds were purchased from TopoGEN, Inc. (Columbus, OH). The testing of the compounds was performed using a commercially available hTopo-IIα drug screening kit. All the synthesized compounds and etoposide were dissolved in DMSO at a concentration of 1 mM as a stock solution and stored at −20 °C.

4.3.4. TopoII-mediated DNA decatenation assay

In agarose gel decatenation assay, kinetoplast DNA (kDNA) was used as a substrate. All the reactions were assembled on ice in micro centrifuge tubes. Briefly, 2–4 units of purified human topoisomerase II, 150 ng catenated DNA (kDNA), and 100 μM drug dissolved in DMSO were combined in freshly prepared 5× complete reaction buffer. The reaction mixture was brought to a final volume of 20 μL with deionized, distilled H_2O. For the standard assay method, the order of addition to the assay was H_2O, 5× assay buffer (buffer A: 0.5 M Tris–HCl (pH 8), 1.50 M sodium chloride, 100 mM magnesium chloride, 5 mM dithiothreitol, 300 μg of bovine serum albumin/mL; buffer B: 20 mM ATP in water), kDNA, followed by either test compound or standard drug and finally topoisomerase II. The reaction mixture was incubated at 37 °C for 30 min. The reaction was then stopped with 10% SDS, followed by digestion with proteinase K and further incubated at 37 °C for 15 min. Topological forms of kDNA were resolved by running 1% agarose gel electrophoresis in Tris–acetate–EDTA (TAE) buffer containing 0.5 μg/mL ethidium bromide and further destained with water for 20 min. The bands of kDNA and decatenated products were visualized by UV *trans*-illumination, and the products were quantified with Image Lab (BioRad).

4.3.5. Topo I mediated DNA relaxation assay

Synthesized compound was screened for hTopo I mediated DNA relaxation assay as follows. Reaction mixture containing freshly prepared 10× reaction assay buffer (100 mM Tris–HCl (pH-7.9), 10 mM EDTA, 1.5 M sodium chloride, 1% BSA, 1 mM spermidine,

50% glycerol) 250 ng supercoiled DNA (substrate), 100 μM camptothecin or investigational compound dissolved in DMSO followed by addition of purified hTopo-I were incubated at 37 °C for 30 min. The reaction was terminated with the addition of 10% SDS, followed by digestion with proteinase K. Further the reaction mixture was again incubated at 70 °C for 15 min. each sample was then subjected to 1% agarose gel electrophoresis in Tris–acetate–EDTA (TAE) buffer containing 0.5 μg/mL ethidium bromide and further destained with water for 20 min. The bands were analyzed under UV *trans*-illuminator and the nicked and relaxed products were quantified with Image Lab (BioRad).

4.4. Molecular docking

3D co-crystal structures of human topoisomerase IIα (PDB entry: 1ZXM)[31] was obtained from protein data bank. Human topoisomerase IIα is a homodimer consisting of two identical subunits, each contains AMPPNP (50-adenylyl-*b*,*c*-imidodiphosphate) and Mg^{2+} ion at the ATP binding pocket. GLIDE 6.1 module of Schrödinger Suite. *E*-Configuration of **ARK-4** was drawn in ChemBio3D Ultra 12.0 and energy minimization was done using the MM2 force field. The ligands were prepared by LIGPREP module. The protein preparation was carried out using Prep Wiz. The protein was first pre-processed and the missing side chain and loops were filled using PRIME. The metal binding states were generated and the protein was then optimized and minimized. The grid box was generated around the centroid of the co-crystallized ligand at the ATP binding site. The docking was carried out using GLIDE XP module. Post docking minimization was performed and up to ten poses per ligand were included.

Acknowledgments

R.K. and S.S. thank DST and UGC, New Delhi, India for the financial assistance (F. No. SR/FT/CS-71/2011) and F.30-13/2013(BSR), respectively. S.M.A., A.T.B. and U.C.B. gratefully acknowledge the financial aid from DBT Government of India, New Delhi to carry out hTopoI and hTopoII activity evaluation studies. J.M.A. and R.K. also thank Maulana Azad National Fellowship (F1-17.1/2013-14/MANF-2013-14-CHR-DEL-27187) for the same. Encouragement and support from Prof. P. Ramarao, Dean, and Prof. R.K. Kohli, Vice Chancellor Central University of Punjab, is gratefully acknowledged.

Supplementary data

Supplementary data associated with this article can be found, in the online version, at http://dx.doi.org/10.1016/j.bmc.2015.07.020.

References and notes

1. Hanahan, D.; Weinberg, R. A. *Cell* **2011**, *144*, 646.
2. Rana, A.; Alex, J. M.; Chauhan, M.; Joshi, G.; Kumar, R. *Med. Chem. Res.* **2015**, *24*, 903.
3. Muregi, F. W.; Ishih, A. *Drug Dev. Res.* **2010**, *71*, 20.
4. Baviskar, A. T.; Banerjee, U. C.; Gupta, M.; Singh, R.; Kumar, S.; Gupta, M. K.; Kumar, S.; Raut, S. K.; Khullar, M.; Singh, S.; Kumar, R. *Bioorg. Med. Chem.* **2013**, *21*, 5782.
5. Alex, J. M.; Singh, S.; Kumar, R. *Arch. Pharm.* **2014**, *347*, 717.
6. Chauhan, M.; Rana, A.; Alex, J. M.; Negi, A.; Singh, S.; Kumar, R. *Bioorg. Chem.* **2015**, *58*, 1.
7. Kaur, G.; Cholia, R. P.; Mantha, A. K.; Kumar, R. *J. Med. Chem.* **2014**, *57*, 10241.
8. Kumar, S.; Sapra, S.; Kumar, R.; Gupta, M. K.; Koul, S.; Kour, T.; Saxena, A. K.; Suri, O. P.; Dhar, K. L. *Med. Chem. Res.* **2012**, *21*, 3720.
9. Negi, A.; Ramarao, P.; Kumar, R. *Mini Rev. Med. Chem.* **2013**, *13*, 653.
10. Malhi, S. S.; Budhiraja, A.; Arora, S.; Chaudhari, K. R.; Nepali, K.; Kumar, R.; Sohi, H.; Murthy, R. S. *Int. J. Pharm.* **2012**, *432*, 63.
11. Shen, T.; Wang, X.-N.; Lou, H.-X. *Nat. Prod. Rep.* **2009**, *26*, 916.
12. Cragg, G. M.; Kingston, D. G.; Newman, D. J. *Anti. Cancer Agents Med. Chem.*; CRC PressI Llc, 2012.
13. Colin, D.; Gimazane, A.; Lizard, G.; Izard, J. C.; Solary, E.; Latruffe, N.; Delmas, D. *Int. J. Cancer* **2009**, *124*, 2780.
14. Piotrowska, H.; Myszkowski, K.; Ziółkowska, A.; Kulcenty, K.; Wierzchowski, M.; Kaczmarek, M.; Murias, M.; Kwiatkowska-Borowczyk, E.; Jodynis-Liebert, J. *Toxicol. Appl. Pharmacol.* **2012**, *263*, 53.
15. Asano, T.; Yoshikawa, T.; Usui, T.; Yamamoto, H.; Yamamoto, Y.; Uehara, Y.; Nakamura, H. *Bioorg. Med. Chem.* **2004**, *12*, 3529.
16. Shao, T.; Wang, J.; Chen, J.-G.; Wang, X.-M.; Li, H.; Li, Y.-P.; Li, Y.; Yang, G.-D.; Mei, Q.-B.; Zhang, S.-Q. *Eur. J. Med. Chem.* **2014**, *75*, 96.
17. Marks, P. A.; Rifkind, R. A.; Richon, V. M.; Breslow, R. *Clin. Cancer Res.* **2001**, *7*, 759.
18. Simonini, M.; Camargo, L.; Dong, E.; Maloku, E.; Veldic, M.; Costa, E.; Guidotti, A. *Proc. Natl. Acad. Sci. U.S.A.* **2006**, *103*, 1587.
19. Kamal, A.; Rao, A. S.; Nayak, V. L.; Reddy, N. S.; Swapna, K.; Ramakrishna, G.; Alvala, M. *Org. Biomol. Chem.* **2014**, *12*, 9864.
20. Rilova, E.; Erdmann, A.; Gros, C.; Masson, V.; Aussagues, Y.; Poughon-Cassabois, V.; Rajavelu, A.; Jeltsch, A.; Menon, Y.; Novosad, N. *ChemMedChem* **2014**, *9*, 590.
21. Kumar, R.; Ujjinamatada, R. K.; Hosmane, R. S. *Org. Lett.* **2008**, *10*, 4681.
22. Correia, C.; Leite, C.; Proença, M. F.; Carvalho, M. A. *Bioorg. Med. Chem. Lett.* **2014**, *24*, 2768.
23. Kumar, D.; Jadhavar, P. S.; Nautiyal, M.; Sharma, H.; Meena, P. K.; Adane, L.; Pancholia, S.; Chakraborti, A. K. R. *Soc. Chem. Adv.* **2015**, *5*, 30819.
24. Qin, J.; Huang, L.; Cao, Y.; Sun, Z. R. *Soc. Chem. Adv.* **2015**, *5*, 7291.
25. Zhang, H.; Jiang, L. *Tetrahedron Lett.* **2015**, *56*, 2777.
26. Kumar, D.; Kumar, R. *Tetrahedron Lett.* **2014**, *55*, 2679.
27. Mavandadi, F.; Lidstrom, P. *Curr. Top. Med. Chem.* **2004**, *4*, 773.
28. Hande, K. *Eur. J. Cancer* **1998**, *34*, 1514.
29. Baviskar, A. T.; Madaan, C.; Preet, R.; Mohapatra, P.; Jain, V.; Agarwal, A.; Guchhait, S. K.; Kundu, C. N.; Banerjee, U. C.; Bharatam, P. V. *J. Med. Chem.* **2011**, *54*, 5013.
30. Baviskar, A. T.; Amrutkar, S. M.; Trivedi, N.; Chaudhary, V.; Nayak, A.; Guchhait, S. K.; Banerjee, U. C.; Bharatam, P. V.; Kundu, C. N. *ACS Med. Chem. Lett.* **2015**, *6*, 481.
31. Wei, H.; Ruthenburg, A. J.; Bechis, S. K.; Verdine, G. L. *J. Biol. Chem.* **2005**, *280*, 37041.
32. Pommier, Y.; Leo, E.; Zhang, H.; Marchand, C. *Chem. Biol.* **2010**, *17*, 421.